EC Accepts, published online ahead of print on 13 June 2008
Eukaryotic Cell doi:10.1128/EC.00109-08

CONTRIBUTION OF GALACTOFURANOSE TO THE VIRULENCE OF THE OPPORTUNISTIC PATHOGEN *ASPERGILLUS FUMIGATUS*

Running Title: *A. fumigatus* UDP-galactopyranose mutase

Philipp S. Schmalhorst[1], Sven Krappmann[2a], Wouter Vervecken[3], Manfred Rohde[4], Meike Müller[5], Gerhard H. Braus[2], Roland Contreras[3], Armin Braun[5], Hans Bakker[1] and Françoise H. Routier[1*]

[1] Department of Cellular Chemistry, Hannover Medical School, Hannover, Germany

[2] Department of Molecular Microbiology and Genetics, Georg-August-University, Göttingen, Germany

[3] Department of Molecular Biology, Ghent University and Department for Molecular Biomedical Research, VIB, Ghent, Belgium

[4] Department of Microbial Pathogenicity, Helmholtz Centre for Infection Research, Braunschweig, Germany

[5] Department of Immunology, Allergology and Immunotoxicology, Fraunhofer Institute of Toxicology and Experimental Medicine, Hannover, Germany

[*]Corresponding author. Department of Cellular Chemistry (OE 4330), Hannover Medical School, 30625 Hannover, Germany. Phone: +49 (511) 532-9807. Fax: +49 (511) 532-3956. E-mail: Routier.Francoise@mh-hannover.de

[a] Present address: Research Center for Infectious Diseases, Würzburg, Germany

ABSTRACT

The filamentous fungus *Aspergillus fumigatus* is responsible for a lethal disease called invasive aspergillosis that affects immunocompromised patients. This disease, like other human fungal diseases, is generally treated by compounds targeting the primary fungal cell membrane sterol. Recently, glucan synthesis inhibitors were added to the limited antifungal arsenal and encouraged the search for novel targets in cell wall biosynthesis. Although it is a major component of *A. fumigatus* cell wall and extracellular matrix, the biosynthesis and role of galactomannan are currently unknown. By a targeted gene deletion approach, we demonstrate that UDP-galactopyranose mutase, a key enzyme of galactofuranose metabolism, controls the biosynthesis of galactomannan and galactofuranose containing glycoconjugates. The *glfA* deletion mutant generated in this study is devoid of galactofuranose and displays attenuated virulence in a low dose mouse model of invasive aspergillosis that likely reflects the impaired growth of the mutant at mammalian body temperature. Furthermore, the absence of galactofuranose results in a thinner cell wall that correlates with an increased susceptibility to several antifungal agents. The UDP-galactopyranose mutase appears thus as an appealing adjunct therapeutic target in combination with other drugs against *A. fumigatus.* Its absence from mammalian cells offers indeed a considerable advantage to achieve therapeutic selectivity.

INTRODUCTION

The filamentous fungus *Aspergillus fumigatus* is the primary cause of invasive aspergillosis, an often fatal condition affecting people with a weakened immune system. Along with the immunocompromised population, the incidence of invasive aspergillosis is constantly growing but therapy remains problematic. The sterol binding polyene amphotericin B and ergosterol biosynthesis inhibitor itraconazole have long been the drugs of choice for treatment of this infection. But because of their higher efficacy and lower toxicity, new triazoles such as voriconazole or posaconazole are supplanting these drugs (28,33). Additionally, a novel class of antifungal agents called the echinocandins provides further options for treatment. These compounds inhibit the synthesis of β1,3-glucan, a major cell wall component with resultant osmotic instability and lysis (12). Their minimal toxicity and synergistic activity with voriconazole and amphotericin B make them particularly attractive for combination therapy although clinical validation is still awaited (35,33). Despite these advances in therapy, invasive aspergillosis is often associated with significant morbidity and mortality emphasizing the need for novel therapeutic strategies based on the fundamental knowledge of *A. fumigatus* pathogenesis.

The development of echinocandins illustrates the viability of targeting enzymes involved in cell wall biosynthesis and encourages the development of chitin synthesis inhibitors. Like glucan and chitin, galactomannan is an abundant component of *A. fumigatus* cell wall (4). This polysaccharide composed of a linear mannan core branched with short β1,5-linked galactofuranose (Gal*f*) chains (22) is covalently bound to the cell wall β1,3-glucan, anchored to the lipid membrane by a glycosylphosphatidylinositol (GPI), or released in the environment during tissue invasion or growth in culture (3,9,14). Besides being an abundant component of the extracellular matrix, secreted galactomannans are used for serological diagnostic of invasive

aspergillosis (1). The monosaccharide Gal*f* has also been reported in the N- and O-glycans of some glycoproteins as well as the glycosphingolipids of *A. fumigatus* (47,29,23,41) and represents thus an important constituent of this fungus cell wall. Gal*f* is otherwise infrequent in natural compounds but prevalent in pathogens. Moreover since it is absent from higher eukaryotes and involved in the survival or virulence of various bacteria, the enzymes involved in the biosynthesis of Gal*f* are considered as attractive drug targets (32,34).

Our understanding of Gal*f* metabolism in eukaryotes is limited. Gal*f* is most likely incorporated into cell surface components by specific galactofuranosyltransferases using UDP-Gal*f* as donor. The work of Trejo and colleagues in early 1970s already suggested the existence of an enzyme converting UDP-galactopyranose into UDP-galactofuranose involved in the biosynthesis of fungal cell wall (48). This enzyme named UDP-galactopyranose mutase (UGM) and encoded by the *glf* gene was first described in bacteria (17,50,30) and lately in several eukaryotic pathogens including *A. fumigatus* (2,5). UGM is to date the only characterised enzyme involved in the biosynthesis of galactofuranose containing molecules in eukaryotes whereas several galactofuranosyltransferases have been described in bacteria (15,19,51,27). The identification of this enzyme, highly conserved amongst lower eukaryotes and present in many fungi, enables studies on the biological role of galactofuranose in these organisms. The present report highlights the role of galactofuranose in *Aspergillus fumigatus* growth and virulence.

MATERIAL AND METHODS

Strains, media and growth conditions. *Aspergillus fumigatus* clinical isolate D141 (38) was used as wild type strain in this study. All strains were grown at 37 °C on Aspergillus minimal medium (AMM) containing 1 % D-glucose as carbon source and 70 mM $NaNO_3$ as nitrogen source (36) unless otherwise stated. Phleomycin or 5-fluoro-2'-deoxyuridine (FUDR) were added for selection purposes at 30 µg/mL and 100 µM respectively.

Generation of *A. fumigatus* mutant strains. The 5' and 3' flanking regions (1.5 and 2 kb respectively) of *A. fumigatus glfA* coding sequence were amplified from genomic DNA by PCR with primers PS12/PS1 and PS3/PS4 (Table 1) respectively and cloned into the pBluescript II SK(-) vector (Stratagene) using the restriction sites SacII/NotI and EcoRV/ClaI. A SpeI/NotI fragment released from pSK269 containing the phleo/tk blaster (18) was then inserted between the two fragments to obtain the disruption plasmid pΔglfA. For reconstitution of the *glfA* gene locus, the plasmid pglfA* was constructed as follows. The phleo/tk blaster of pΔglfA was first replaced with the original *A. fumigatus glfA* gene by homologous recombination in *E. coli* strain YZ2000 (Gene Bridges, Leimen, Germany). A single point mutation was introduced by site-directed mutagenesis. Briefly, non-methylated plasmid DNA was generated from a methylated parent plasmid by Phusion DNA-Polymerase (NEB) using complementary primers that both carried the desired mutation (PS23s/PS23r, Table 1). Prior to transformation the parental, methylated DNA strand was specifically cleaved by DpnI to selectively obtain transformants that harbored the mutated plasmid. Thus, codon 130 of *glfA* coding sequence (GenBank Accession number AJ871145) was changed from CTT to CTC which generated a new XhoI restriction site. Since gene reconstitution by homologous recombination could not be obtained with this

construct, 5' and 3' flanking regions were extended to 5 kb by replacement with re-cloned PCR fragments (primer pairs PS28/PS1 and PS3/PS31) to obtain the final pglfA* construct.

The pΔglfA and pglfA* plasmids were linearised (KpnI/SacII) before polyethylene glycol-mediated fusion of protoplasts as described in (37). Transformants were grown on AMM plates containing 1.2 M sorbitol as osmotic stabiliser under appropriate selection conditions and singled out twice before further analysis. Accurate gene deletion and reconstitution were confirmed by southern hybridisation. Southern probes were amplified from genomic DNA using primer pairs PS66A/PS67A, PS68A/PS69A and PS20/PS21. All primer sequences are provided in Table 1.

Western Blots. Cell wall glycoproteins and soluble polysaccharides were extracted from 30 mg ground *A. fumigatus* mycelium by incubation in 1 mL sample buffer (15 % glycerol, 100 mM Tris/HCl pH 6.8, 1.5 % SDS, 0.25 % β-mercaptoethanol, 0.025 % bromophenol blue) for 12 min at 95 °C. 20 µl of the supernatant were separated on a 10 % SDS-polyacrylamide gel and transferred to nitrocellulose membranes. The monoclonal antibody EB-A2 (42) conjugated to horseradish peroxidase (HRP) from the Platelia *Aspergillus* Test (Bio-Rad, Hercules, CA, USA) or HRP-coupled lectin Concanavalin A (ConA, Sigma-Aldrich) were used in a 1:50 dilution or at 0.2 µg/mL respectively. HRP activity was visualised by an enhanced chemiluminescence system (Pierce**,** Rockford, IL, USA).

N-glycan analysis. N-glycans of secreted glycoproteins in the supernatant of an *A. fumigatus* liquid culture were analyzed after Peptide N-Glycosidase F (PNGase F) mediated release and 8-amino-1,3,6-pyrenetrisulfonic acid (APTS) labeling by capillary electrophoresis as recently described (20). Separation was carried out on a 4-capillary electrophoresis DNA Sequencer

(3130 Genetic Analyzer, Applied Biosystems, Foster City, CA, USA). Oligomaltose and bovine RNAse B N-glycans (Prozyme, San Leandro, CA, USA) served as reference oligosaccharides.

Purification and analyis of glycosylinositolphosphoceramides (GIPCs). Mycelia (0.5 g) ground in liquid nitrogen with a mortar and pestle were disrupted by sonication in 6 mL of $CHCl_3$/MeOH 1:1. After addition of 3 mL $CHCl_3$ (to obtain a $CHCl_3$/MeOH ratio of 2:1), GIPCs were extracted at room temperature for at least 15 min on a rotating shaker. 3 mL MeOH were then added to lower the density and the mixture centrifuged for 10 min at 2000 g to remove insoluble material. Chloroform and H_2O were then added to the supernatant to obtain a biphasic system with an 8/4/3 ratio of $CHCl_3$/MeOH/H_2O. After centrifugation for 10 min at 2000 g, GIPCs contained in the upper phase were collected and applied to a C18/SepPak cartridge (Waters, Eschborn, Germany) pre-equilibrated with 5 mL $CHCl_3$/MeOH/H_2O 3/48/47. After washing of the column with 20 mL $CHCl_3$/MeOH/H_2O 3/48/47, glycolipids were eluted with 5 mL methanol and dried under a stream of nitrogen. High performance thin layer chromatography and immunostaining with the monoclonal antibody MEST-1 were carried out as previously described (47).

Growth assay. For radial growth measurement, a 10 µl drop containing 10,000 *A. fumigatus* conidia was placed in the centre of an agar plate containing either minimal (AMM) or complete medium (potato dextrose agar, Becton Dickinson Difco, Heidelberg, Germany). Plates were incubated at various temperatures and colony diameters were measured twice daily.

Antifungal susceptibility testing. The reference broth microdilution test was applied for *A. fumigatus* antifungal susceptibility testing (21). Each antifungal stock was diluted in 200 µl

double-strength RPMI 2%G (RPMI 1640 liquid medium buffered with 165 mM 4-Morpholinepropanesulfonic acid (MOPS) to pH 7.0 and supplemented with 2 % glucose) to obtain the highest concentration to be tested. Nine serial 1:2 dilutions in double-strength RPMI 2%G were made and to each dilution an equal volume (100 µl) of an *A. fumigatus* spore solution ($2.5 \cdot 10^5$/mL in water) was added. Microtitre plates were incubated at 35 °C and fungal growth in each well was read out visually after three days and compared to control wells that contained no antifungal.

Field emission scanning electron microscopy. For morphological studies and measurements of the cell wall thickness *A. fumigatus* wild type and Δ*glfA* mutant mycelium were fixed in 5 % formaldehyde and 2 % glutaraldehyde in cacodylate buffer (0.1 M cacodylate, 0.01 M $CaCl_2$, 0.01 M $MgCl_2$, 0.09 M sucrose, pH 6.9) for 1 h on ice. Samples were washed several times with cacodylate buffer and subsequently with TE-buffer (20 mM Tris/HCl, 1 mM EDTA, pH 6,9) before dehydration in a graded series of acetone (10, 30, 50, 70, 90, 100 %) on ice for 15 min per step. Samples in the 100 % acetone step were allowed to reach room temperature before another change in 100 % acetone. Samples were then subjected to critical-point drying with liquid CO_2 (CPD 30, Balzers, Liechtenstein). Dried samples were then mounted onto conductive carbon adhesive tabs on an aluminium stub and sputter coated with a thin gold film (SCD 40, Balzers Union, Liechtenstein). For cell wall thickness measurements mycelium was fractured by pressing another conductive carbon adhesive tab covered stub onto the sample and separating both stubs immediately thereafter. Fractured hyphae were also made conductive by sputter coating with a gold film before examination in a field emission scanning electron microscope (Zeiss DSM 982 Gemini) using the Everhart Thornley SE-detector and the inlens SE-detector in a 50:50 ratio at an acceleration voltage of 5 kV and at calibrated magnifications.

Mouse infection model. A low-dose mouse infection model of Invasive Aspergillosis for Balb/c mice which had been established previously (25) was essentially used. Immunosuppressive state was established by intraperitoneal injections of 100 mg/kg cyclophosphamide (Endoxan, Baxter Chemicals) on days -4, -1, 0, 2, 5, 8 and 11 and a single subcutaneous dose (200 mg/kg) of a cortisone acetate suspension (Sigma) on day -1. Groups of 20 mice were infected intranasally with 20,000 conidia of wt, Δ*glfA* or *glfA** strain on day 0. The control group received PBS only. Survival was monitored for 13 days after infection and moribund animals were sacrificed. Coincidence of severely reduced mobility, low body temperature and breathing problems was defined as moribundity criterion. Statistical analysis of survival data was carried out using the logrank test implemented in Prism 4 (GraphPad Software, San Diego, CA, USA). For quantification experiments, groups of three to five animals were killed two, four and six days after infection and lungs were removed for further analysis.

Lung histology.

Female Balb/c mice were immunosuppressed and infected as described above. The animals were killed after 5 days and their lungs removed and fixed in 4 % PBS-buffered paraformaldehyde over night. Tissue samples were dehydrated through a series of graded alcohols, cleared with xylene and embedded in paraffin. Tissue sections (5 µm) were stained with either hematoxylin/eosin or by the Periodic Acid Schiff (PAS) method for visualization of fungal cell walls. Photomicrographs were taken with an Axiovert 200 M microscope (Zeiss, Germany) at 10x and 20x magnification.

Preparation of genomic DNA from mouse lungs. Tissue homogenisation was modified according to (7). Immediately after removal, mouse lungs were transferred to a 2 mL screw-cap

containing 1.4 mm ceramic beads (Lysing matrix D, Qbiogene, Irvine, CA, USA) and 20 % glycerol/PBS. Tissue was disrupted using a FastPrep FP120 instrument (Qbiogene) for 3 times 30 seconds at speed 5 with intermediate cooling on ice. The disrupted tissues were further homogenised with approx. 250 mg acid-washed glass beads (0.45-0.5 mm, Sigma-Aldrich) by vortexing three times for 30 s with intermediate cooling on ice. The DNeasy Blood & Tissue Kit (Qiagen, Hilden, Germany) was used to extract genomic DNA from an equivalent of 8 % of the starting tissue material of this homogenate. DNA was finally recovered in 200 µl elution buffer.

Quantitative PCR (qPCR). Quantitative PCR was carried out essentially as described previously (7). Primers for amplification of a 18S rRNA gene (GenBank Accession number AB008401) fragment specific for *A. fumigatus* and a hybridisation probe labeled with carboxyfluorescein (FAM; 5' end) and carboxytetramethylrhodamine (TAMRA; 3' end) were designed using Primer Express software version 3.0 (Applied Biosystems; Table 1). qPCR reactions were performed in a 7500 Fast Real-Time PCR System instrument (Applied Biosystems) loaded with MicroAmp optical 96-well plates sealed with Optical Adhesive Cover (Applied Biosystems). Each qPCR reaction (20 µl) contained 5 µl sample DNA, 250 nM dual-labeled hybridisation probe, 500 nM primers, 250 µg/mL BSA and TaqMan Fast Universal Master Mix (Applied Biosystems) containing dNTPs, buffer and the fluorescent dye carboxyrhodamine (ROX) as a passive reference. Real-time PCR data was acquired using Sequence Detection Software v1.3.1. FAM/ROX fluorescence ratio was recorded at every cycle and a C_T value was assigned to each reaction, defining the cycle number at which the FAM/ROX signal surpassed an automatically defined threshold. C_T values were corrected for differences in yield of genomic DNA by normalization to DNA concentration of a control sample using the formula $C_{T,norm} = C_{T,measured} + \log_2([DNA]_{sample} / [DNA]_{control})$ (7). Translation of sample $C_{T,norm}$

values into rDNA gene copy numbers was done as follows: C_T values of serial 1:10 dilutions containing N = 300 to 300,000 molecules (calculated from M_w and DNA concentration determined by OD_{260}) of a plasmid bearing the cloned *A. fumigatus* 18S rDNA gene were plotted against N to generate a calibration curve which was then used to assign a rDNA copy number to a given sample $C_{T,norm}$ value. Conidial equivalents were calculated from gene copy numbers by means of uninfected tissue samples that were spiked with defined numbers of conidia before tissue homogenisation (7). Samples, controls and standards were analyzed in triplicates.

RESULTS

Deletion and reconstitution of the *glfA* gene in *A. fumigatus*. To begin investigating the role of Gal*f* in *Aspergillus fumigatus* biology, we deleted the gene encoding UGM (GenBank locus tag AJ871145) and named it *glfA* following the recommendations for gene naming in *Aspergillus*. To do this, we generated a deletion plasmid containing the regions flanking the *glfA* coding sequence separated by the bifunctional selection cassette phleo/tk that confers both resistance to phleomycin and sensitivity to 5-fluoro-2'-deoxyuridine (FUDR) (18). This construct was used to transform protoplasts of *A. fumigatus* clinical strain D141 which served as wild type (wt) and phleomycin resistant transformants were analyzed by Southern Blot using several digoxigenin-labeled probes (Fig. 1). One of the clones that had undergone the desired gene replacement (Fig. 1) was selected for further analysis and named Δ*glfA*.

The selected disruptant was further subjected to protoplast transformation with a large DNA fragment encompassing the *glfA* coding sequence which contained a single translationally silent nucleotide exchange that generated an XhoI restriction site. Gene replacement in the transformants resulted in the reconstitution of the *glfA* locus (Fig. 1) as detected by FUDR resistance and proven by Southern Blot analysis for a selected clone named *glfA** (Fig. 1B). The silent mutation introduced in the reconstituted strain allowed differentiating between wild type and *glfA** as demonstrated in figure 1B (top) and thus enabled us to rule out contamination by the wt strain. The reconstitution of the *glfA* locus ensures that any phenotype observed in the Δ*glfA* strain can be reverted and hence be securely attributed to the loss of the *glfA* gene.

Gal*f* is absent from the *A. fumigatus ΔglfA* mutant. To confirm that deletion of *glfA* indeed altered the expression of Gal*f* containing glycoconjugates, aqueous mycelial extracts were tested for reactivity to the Gal*f*-specific monoclonal antibody (mAb) EB-A2. This antibody recognizes

preferably β1,5-linked Gal*f*-residues that are present in all forms of galactomannan (cell-wall bound, membrane bound or secreted) (42) as well as in some O-glycans (23). Moreover a second binding epitope, Gal*f*(β1,2)Man, which is part of galactofuranosylated N-glycans has been postulated (29). Thus, EB-A2 can be used to simultaneously detect galactomannan and galactofuranosylated glycoproteins. Western blot analysis of wt and *glfA** total mycelial extracts labeled with horseradish peroxidase (HRP) conjugated EB-A2 revealed a smear migrating around 40 to 80 kDa in accordance with previous findings (42). In contrast, the Δ*glfA* mycelial extract was not stained at all, indicating absence of Gal*f* in the galactomannan and glycoproteins of this mutant (Fig. 2A, left). In contrast, Concanavalin A (ConA) used as loading control bound slightly better to the Δ*glfA* extract than to those of wt and *glfA** (Fig. 2A, right). The lack of Gal*f* in the Δ*glfA* mutant might increase the accessibility of the mannan for ConA and thus could explain this finding.

Similarly, the absence of Gal*f* in Δ*glfA* glycolipids was shown by the absence of reactivity to the monoclonal antibody MEST-1. This antibody that recognizes β1,3- and β1,6-linked Gal*f* residues (43) labeled several *A. fumigatus* glycosylinositolphosphoceramides (GIPCs) after separation by high-performance thin layer chromatography as previously shown (47) but did not label glycosphingolipids extracted from the Δ*glfA* mutant (Fig. 2B, left). The upper bands observed in this panel might be attributed to GIPCs containing 1 or 2 Gal*f* and 2 or 3 mannose residues as recently described (41,47). In addition, Simenel et al. reported an unusual GIPC containing a Gal*f* residue substituted by a choline phosphate. The lower band present in the wt chromatogram could correspond to a similar GIPC. Staining of glycolipids by orcinol was used as loading control (Fig. 2B, right). The simpler Δ*glfA* chromatogram is compatible with the absence of Gal*f* containing GIPCs. The uppermost band observed in the chromatogram most probably correspond to Man(α1,3)Man(α1,2)Ins-P-Cer while the band just beneath could be attributed to

Man(α1,2)Man(α1,3)Man(α1,2)Ins-P-Cer (47). The chromatograms obtained from the reconstituted mutant *glfA** and wt were undistinguishable (data not shown).

Additionally, N-glycans enzymatically released from *A. fumigatus* secreted proteins were analyzed by capillary electrophoresis after fluorescent labeling (20,8). The profiles obtained are presented in figure 3A (panels 1 and 2). The peaks labeled 1, 2, 3, 4 and 5 present in both electropherograms co-migrated with reference oligosaccharides M5 to M9 (Fig. 3A; panel 9 and Fig. 3B). Moreover, digestion of these N-glycans by *Trichoderma reesei* α1,2-mannosidase indicates that 2, 3, 4 and 5 arise from substitution of oligosaccharide 1 with one to four mannose residues linked in α1,2 (Fig. 3A; panels 3 and 4). The profile obtained with wt N-glycans (Fig. 3A; panel 1) presents four additional peaks labeled 1a, 2a, 3a and 4a that were absent from *glfA* N-glycans. The retention times of these peaks suggest that they arise from substitution of oligosaccharides 1-4 with a single Gal*f* residue. The presence of a terminal non-reducing Gal*f* residue in *A. fumigatus* N-glycans has been previously reported (9) and was demonstrated by hydrofluoric acid (HF) treatment of the N-glycans after *Trichoderma reesei* α1,2-mannosidase digestion (Fig. 3A, panels 5 and 6). This mild acid treatment, known to release Gal*f*, entirely converted oligosaccharide 1a into oligosaccharide 1 (Fig. 3A; panels 3 and 5). In contrast, HF treatment did not change the profile of Δ*glfA* N-glycans digested with α1,2 mannosidase (Fig. 3A, panels 4 and 6).

Interestingly, the comparison of wt and Δ*glfA* N-glycans digested with *T. reesei* α1,2 mannosidase or Jack Bean mannosidase helps positioning the Gal*f* residue. Alpha1,2-mannosidase treatment converted the oligosaccharides 2a, 3a and 4a into 1a while the oligosaccharides 2, 3 and 4 generated 1 (Fig. 3A; compare panels 1 and 2 with 3 and 4). This indicates that the Gal*f* residue does not protect any mannose residues from the exomannosidase digestion and thus does not substitute an α1,2-linked mannose (Fig. 3A; panels 3 and 4).

Moreover, Jack Bean mannosidase digestion of wt N-glycans resulted in a major peak (peak 7), attributed to Gal*f*$Man_3GlcNAc_2$ from its retention time, in addition to $Man_1GlcNAc_2$ (peak 6) expected from digestion of high-mannose type N-glycans (Fig. 3A; panels 7 and 8). These experiments do not allow for the determination of the detailed N-glycan structure but suggest that they resemble the N-glycans of *A. niger* α-glucosidase and α-galactosidase (44,45). More importantly, these experiments demonstrate the absence of Gal*f* in the Δ*glfA* N-glycans.

Loss of Gal*f* alters morphology and growth of *A. fumigatus*. The Δ*glfA* strain exhibited a marked growth defect on solid minimal media or complete media when compared to wt. This effect could be observed for a wide range of temperatures (Fig. 4) and was statistically different in all cases ($P < 0.001$, *t* test, $n = 3$). The most severe effect was found at 42 °C with a 75 % reduction in radial growth (Fig. 4C). In parallel, Δ*glfA* conidiation was diminished by 90 % at 37 °C and was almost absent at 42 °C. In contrast, the onset and rate of germination of wt, Δ*glfA* and *glfA** conidia were similar. In minimal media at 37 °C, the conidia of all strains started forming germ tubes at 3.2 h and reached 100 % germination within 8 to 9 h (data not shown). Scanning electron micrographs of intact mycelium, conidiophores and conidia of Δ*glfA* did not reveal any obvious morphologic differences. However, the observation of fractured mycelium revealed a marked reduction of the Δ*glfA* cell wall thickness (Fig. 5). Measurements indicated that the cell wall of wt *A. fumigatus* varies from 85 to 315 nm which is in good agreement with earlier findings (39). In contrast, Δ*glfA* cell wall thickness ranged from 85 to 150 nm. The mean values (± standard deviation) of cell wall thickness obtained from 25 measurements were 227.5 nm (± 15.98 nm) and 109.7 nm (± 11.3 nm) for wt and Δ*glfA* hyphae respectively. The cell wall of Δ*glfA* was thus approximately half the thickness of the wild type cell wall.

***ΔglfA* is more susceptible to drugs.** The structural cell wall defect caused by Gal*f* deficiency was accompanied by an increased susceptibility to several antifungal agents (Table 2). MICs determined in a broth microdilution test were slightly reduced for amphotericin B and caspofungin in the Δ*glfA* mutant. A more pronounced increase in susceptibility was seen for voriconazole (0.04 mg/L for Δ*glfA* compared to 0.3 mg/L for wt) and nikkomycin Z (63-125 mg/L for Δ*glfA* and 500 mg/mL for wt), suggesting an increased permeability of the cell wall caused by the loss of Gal*f*. In contrast, the sensitivity towards oxidative stress remained unchanged as indicated by equal MICs for H_2O_2 in both wt and Δ*glfA*.

Δ*glfA* displays attenuated virulence in a murine model of invasive aspergillosis. The influence of the *glfA* deletion on pathogenicity of *A. fumigatus* was assessed in a low-dose infection model of invasive aspergillosis (25). Cyclophosphamide was used to induce neutropenia in female Balb/c mice and a single dose of cortisone acetate was administered before intranasal infection with 20,000 *A. fumigatus* conidia. Neutropenia was maintained throughout the observation period of 13 days and survival was recorded daily (Fig. 6A). 90 % of the animals infected with wt did not survive day seven after infection, whereas half of the mice infected with Δ*glfA* were still alive on day 13. A logrank test on wt and Δ*glfA* survival data confirmed that the observed difference was statistically significant (P = 0.0004). The attenuation in virulence could clearly be attributed to the absence of *glfA*, since animals infected with the reconstituted wild type strain *glfA** showed a survival pattern nearly identical to wt (no significant difference in logrank test, P = 0.559). Histological examination of lung tissue from mice infected with wt, Δ*glfA* and *glfA** 5 days after inoculation showed evident fungal growth surrounding bronchioles and tissue penetration (Fig. 7). For each strain, inflammatory cells were rarely observed at the sites of infection.

To correlate the delay in the onset and progression of mortality with a growth defect, fungal burden in lungs of infected mice was determined by quantitative PCR (Fig. 6B). Mice were treated and infected as described above. After two, four and six days, animals were sacrificed and their lungs taken. DNA was isolated from homogenized lung tissue and fungal content determined by amplification of a part of *A. fumigatus* ribosomal DNA. As shown in figure 6B, growth of Δ*glfA* was restricted *in vivo* when compared to wt, which was in agreement with the slower growth observed *in vitro*.

DISCUSSION

The essential role of the β1,3-glucan in cell wall organization and growth of several pathogenic fungi has been the basis for the development of the echinocandins (11). Likewise, inhibitors of chitin biosynthesis are currently explored as new antifungal drugs since chitin is an important structural element of the fungal cell wall (6). In contrast, although it is a major component of the cell wall and extracellular matrix, the role of galactomannan had not yet been investigated since the enzymes involved in its biosynthesis are unknown. Recently, we and others characterized the UDP-galactopyranose mutase (UGM) of various pathogenic eukaryotes including *A. fumigatus* (2,5). In prokaryotes, like in the protozoan *Leishmania*, this enzyme is the only route to the formation of UDP-Gal*f*, the donor substrate of galactofuranosyltransferases, and thus controls the biosynthesis of all Gal*f* containing molecules. Likewise, *A. fumigatus* UGM was found to be essential for the biosynthesis of galactomannan as well as some glycosphingolipids and glycoproteins. Like in other organisms (16,32), deletion of the *glfA* gene resulted in the complete absence of Gal*f*, as shown for instance by the absence of reactivity to the antibody EB-A2.

Besides demonstrating the lack of Gal*f* in the Δ*glfA* mutant, our analyses provide useful structural information of *A. fumigatus* N-glycans. Treatment of wild type secreted proteins with PNGase F released galactofuranosylated high-mannose type N-glycans. The size of the oligosaccharides and presence of a single Gal*f* residue is in agreement with previous studies in filamentous fungi (26,29). Moreover, analysis of these oligosaccharides after digestion by Jack bean- or *T. reesei* α1,2-mannosidase helps positioning the Gal*f* residue. These data and the comparison with high-mannose standards suggest that the N-glycans from *A. fumigatus* secreted proteins resemble those of *A. niger* α-D-galactosidase and α-D-glucosidase (45,44,49). These N-glycans might have simply arisen from trimming of the $Glc_3Man_9GlcNAc_2$ precursor and substitution by a Gal*f* residue. *Aspergilli* indeed contain several α1,2-mannosidase genes and

trimming of high mannose glycans has been shown previously (52,13). Interestingly, Gal*f* addition has been suggested to act as a stop signal for mannose addition in analogy to the role proposed for α1,3-linked terminal mannose in *Saccharyomyces cerevisiae* (29,49). However, preventing the addition of galactofuranose does not result in an increased size of the oligosaccharides. On the contrary, $Man_5GlcNAc_2$ is the main oligosaccharide found in the Δ*glfA* mutant while Gal*f*$Man_6GlcNAc_2$ is predominant in wild type.

Although *glfA* deletion has been shown to be lethal in *Mycobacterium smegmatis* (32), the *in vitro* viability of *A. fumigatus* Δ*glfA* mutant is unsurprising since Gal*f* occupies a non-reducing terminal position in the molecules of this fungus. Hence, the absence of Gal*f* does not perturb the basic organization of the cell wall, as would the absence of the underlying structures. Nevertheless, it resulted in marked alterations of the cell surface and notably a thinner cell wall as revealed by electron microscopy. The basis of this drastic change is unclear and difficult to attribute to a particular cell wall component since GPI-/cell wall bound galactomannan, N-glycans, O-glycans and GIPCs are affected by Gal*f* deficiency. In other fungi, the loss of terminal sugar residues has sometimes been associated with reduced cell wall strength. For instance, a *Schizosaccharomyces pombe* mutant deficient in cell wall galactosylation displays morphological changes, attenuated growth and a 25-35 % reduction in cell wall thickness (46).

The structural changes originating from the *glfA* deletion are associated with slower growth indicating that Gal*f* plays an important role in *A. fumigatus* morphogenesis. The temperature-sensitive growth defect at higher temperature displayed by the Δ*glfA* mutant is reminiscent to that observed in the Δ*AfPmt1* mutant, a mutant characterized by reduced O-glycosylation (53). Interestingly, an influence of Gal*f* deficiency on the growth rate was also observed in Δ*glfA* mutants of *Aspergillus nidulans* and *Aspergillus niger* (10). Conversely *glfA* deletion had no

effect on the *in vitro* growth of *Leishmania* parasites (16) highlighting that the role of Gal*f* cannot be translated to every Gal*f* containing organism.

The ability to thrive at 37 °C is a characteristic of human pathogens that has been shown to correlate with virulence potential in the case of *A. fumigatus* (31). Consequently, mutations that affect the growth of fungi at mammalian body temperature are commonly associated with attenuated virulence (40). In this study, we observed slower growth of the *A. fumigatus* Δ*glfA* mutant *in vitro* but also *in vivo* using quantitative PCR. In agreement with this observation, the mutant was clearly attenuated in virulence showing a delay in both the onset and progression of mortality when tested in a low dose mouse infection model of invasive aspergillosis. An altered immune response caused by the different cell wall structure of the Δ*glfA* mutant may also contribute to the attenuation in virulence. However, no differences in adherence and uptake of wt and Δ*glfA* conidia by murine bone-marrow derived dendritic cells or in the production of TNF-α or IL-10 by infected murine bone-marrow derived macrophages were observed (K. Kotz, F. Ebel and F.H. Routier, unpublished data).

The value of echinocandins in invasive aspergillosis treatment resides in their synergistic effects with azoles and amphotericin B. Similarly, chitin synthesis inhibitors demonstrate synergy with echinocandins and azoles (24). These synergistic effects that offer new options for combination antifungal therapy are most likely due to greater cell wall permeability. We did note an increase in susceptibility of the Δ*glfA* mutant to several antifungal agents, notably to voriconazole. However, in the liquid culture conditions classically used for antifungal susceptibility testing, the fungus is not surrounded by extracellular matrix. This extracellular matrix that delays the penetration of drug is rich in galactomannan (3) and is probably altered in the Δ*glfA* mutant as suggested by the compact appearance of colonies on agar plates. *In vivo* a greater increase in susceptibility of the Δ*glfA* mutant to drugs would therefore be expected. Besides the attenuated

1 virulence, this suggests that inhibitors of UGM might be useful in antifungal therapy. The
2 absence of Gal*f* biosynthesis in mammals would represent a considerable advantage for the
3 development of antifungal drugs with selective toxicity.

ACKNOWLEDGMENTS

We thank Dr. Florian Länger, Dr. Frank Ebel and Jakob Engel for their help with histopathology, cytokine analysis and glycolipid analysis respectively. Monika Berger, Verena Grosse, Sabine Schild, Olaf Macke and Brigitte Philippens are thanked for excellent technical assistance and Dr. Anita Straus and Dr. Helio Takahashi for the generous gift of MEST-1 monoclonal antibody. We are indebted to Dr. Rita Gerardy-Schahn for her constant support.

REFERENCES

1. **Aquino, V. R., L. Z. Goldani, and A. C. Pasqualotto**. 2007. Update on the contribution of galactomannan for the diagnosis of invasive aspergillosis. Mycopathologia. **163:**191-202.

2. **Bakker, H., B. Kleczka, R. Gerardy-Schahn, and F. H. Routier**. 2005. Identification and partial characterization of two eukaryotic UDP-galactopyranose mutases. Biol. Chem. **386:**657-661.

3. **Beauvais, A., C. Schmidt, S. Guadagnini, P. Roux, E. Perret, C. Henry, S. Paris, A. Mallet, M. C. Prévost, and J. P. Latgé**. 2007. An extracellular matrix glues together the aerial-grown hyphae of *Aspergillus fumigatus*. Cell Microbiol. **9:**1588-1600.

4. **Bernard, M. and J. P. Latgé**. 2001. *Aspergillus fumigatus* cell wall: composition and biosynthesis. Med. Mycol. **39 Suppl 1:**9-17.

5. **Beverley, S. M., K. L. Owens, M. Showalter, C. L. Griffith, T. L. Doering, V. C. Jones, and M. R. McNeil**. 2005. Eukaryotic UDP-galactopyranose mutase (GLF gene) in microbial and metazoal pathogens. Eukaryot. Cell. **4:**1147-1154.

6. **Borgia, P. T. and C. L. Dodge**. 1992. Characterization of *Aspergillus nidulans* mutants deficient in cell wall chitin or glucan. J. Bacteriol. **174:**377-383.

7. **Bowman, J. C., G. K. Abruzzo, J. W. Anderson, A. M. Flattery, C. J. Gill, V. B. Pikounis, D. M. Schmatz, P. A. Liberator, and C. M. Douglas**. 2001. Quantitative PCR assay to measure *Aspergillus fumigatus* burden in a murine model of disseminated aspergillosis: demonstration of efficacy of caspofungin acetate. Antimicrob. Agents Chemother. **45:**3474-3481.

8. **Callewaert, N., S. Geysens, F. Molemans, and R. Contreras**. 2001. Ultrasensitive profiling and sequencing of N-linked oligosaccharides using standard DNA-sequencing equipment. Glycobiology. **11:**275-281.

9. **Costachel, C., B. Coddeville, J. P. Latgé, and T. Fontaine**. 2-12-2005. Glycosylphosphatidylinositol-anchored fungal polysaccharide in *Aspergillus fumigatus*. J. Biol. Chem. **280:**39835-39842.

10. **Damveld, R. A., A. Franken, M. Arentshorst, P. J. Punt, F. M. Klis, C. A. van den Hondel, and A. F. Ram**. 2008. A Novel Screening Method for Cell Wall Mutants in Aspergillus niger Identifies UDP-Galactopyranose Mutase as an Important Protein in Fungal Cell Wall Biosynthesis. Genetics. **178:**873-881.

11. **Denning, D. W.** 2002. Echinocandins: a new class of antifungal. J. Antimicrob. Chemother. **49:**889-891.

12. **Denning, D. W.** 4-10-2003. Echinocandin antifungal drugs. Lancet. **362:**1142-1151.

13. **Eades, C. J. and W. E. Hintz**. 5-9-2000. Characterization of the class I alpha-mannosidase gene family in the filamentous fungus *Aspergillus nidulans*. Gene. **255:**25-34.

14. **Fontaine, T., C. Simenel, G. Dubreucq, O. Adam, M. Delepierre, J. Lemoine, C. E. Vorgias, M. Diaquin, and J. P. Latgé**. 8-9-2000. Molecular organization of the alkali-insoluble fraction of *Aspergillus fumigatus* cell wall. J. Biol. Chem. **275:**27594-27607.

15. **Guan, S., A. J. Clarke, and C. Whitfield**. 2001. Functional analysis of the galactosyltransferases required for biosynthesis of D-galactan I, a component of the lipopolysaccharide O1 antigen of *Klebsiella pneumoniae*. J. Bacteriol. **183:**3318-3327.

16. **Kleczka, B., A. C. Lamerz, G. van Zandbergen, A. Wenzel, R. Gerardy-Schahn, M. Wiese, and F. H. Routier**. 2007. Targeted gene deletion of *Leishmania major* UDP-galactopyranose mutase leads to attenuated virulence. J. Biol. Chem. **282:**10498-10505.

17. **Köplin, R., J. R. Brisson, and C. Whitfield**. 14-2-1997. UDP-galactofuranose precursor required for formation of the lipopolysaccharide O antigen of *Klebsiella pneumoniae* serotype O1 is synthesized by the product of the $rfbD_{KPO1\ gene}$. J. Biol. Chem. **272:**4121-4128.

18. **Krappmann, S., O. Bayram, and G. H. Braus**. 2005. Deletion and allelic exchange of the *Aspergillus fumigatus veA* locus via a novel recyclable marker module. Eukaryot. Cell. **4:**1298-1307.

19. **Kremer, L., L. G. Dover, C. Morehouse, P. Hitchin, M. Everett, H. R. Morris, A. Dell, P. J. Brennan, M. R. McNeil, C. Flaherty, K. Duncan, and G. S. Besra**. 13-7-2001. Galactan biosynthesis in *Mycobacterium tuberculosis*. Identification of a bifunctional UDP-galactofuranosyltransferase. J. Biol. Chem. **276:**26430-26440.

20. **Laroy, W., R. Contreras, and N. Callewaert**. 2006. Glycome mapping on DNA sequencing equipment. Nat. Protoc. **1:**397-405.

21. **Lass-Flörl, C., M. Cuenca-Estrella, D. W. Denning, and J. L. Rodriguez-Tudela**. 2006. Antifungal susceptibility testing in *Aspergillus* spp. according to EUCAST methodology. Medical Mycology. **44:**319-325.

22. **Latgé, J. P., H. Kobayashi, J. P. Debeaupuis, M. Diaquin, J. Sarfati, J. M. Wieruszeski, E. Parra, J. P. Bouchara, and B. Fournet**. 1994. Chemical and immunological characterization of the extracellular galactomannan of *Aspergillus fumigatus*. Infect. Immun. **62:**5424-5433.

23. **Leitão, E. A., V. C. Bittencourt, R. M. Haido, A. P. Valente, J. Peter-Katalinic, M. Letzel, L. M. de Souza, and E. Barreto-Bergter**. 2003. Beta-galactofuranose-containing O-linked oligosaccharides present in the cell wall peptidogalactomannan of *Aspergillus fumigatus* contain immunodominant epitopes. Glycobiology. **13:**681-692.

24. **Li, R. K. and M. G. Rinaldi**. 1999. In vitro antifungal activity of nikkomycin Z in combination with fluconazole or itraconazole. Antimicrob. Agents Chemother. **43:**1401-1405.

25. **Liebmann, B., T. W. Mühleisen, M. Müller, M. Hecht, G. Weidner, A. Braun, M. Brock, and A. A. Brakhage**. 2004. Deletion of the *Aspergillus fumigatus* lysine biosynthesis gene *lysF* encoding homoaconitase leads to attenuated virulence in a low-dose mouse infection model of invasive aspergillosis. Arch. Microbiol. **181:**378-383.

26. **Maras, M., D. van, I, R. Contreras, and C. A. van den Hondel**. 1999. Filamentous fungi as production organisms for glycoproteins of bio-medical interest. Glycoconj. J. **16:**99-107.

27. **Mikusova, K., M. Belanova, J. Kordulakova, K. Honda, M. R. McNeil, S. Mahapatra, D. C. Crick, and P. J. Brennan**. 2006. Identification of a novel galactosyl transferase involved in biosynthesis of the mycobacterial cell wall. J. Bacteriol. **188:**6592-6598.

28. **Mohr, J., M. Johnson, T. Cooper, J. S. Lewis, and L. Ostrosky-Zeichner**. 2008. Current options in antifungal pharmacotherapy. Pharmacotherapy. **28:**614-645.

29. **Morelle, W., M. Bernard, J. P. Debeaupuis, M. Buitrago, M. Tabouret, and J. P. Latgé**. 2005. Galactomannoproteins of *Aspergillus fumigatus*. Eukaryot. Cell. **4:**1308-1316.

30. **Nassau, P. M., S. L. Martin, R. E. Brown, A. Weston, D. Monsey, M. R. McNeil, and K. Duncan**. 1996. Galactofuranose biosynthesis in *Escherichia coli* K-12: identification and cloning of UDP-galactopyranose mutase. J. Bacteriol. **178:**1047-1052.

31. **Paisley, D., G. D. Robson, and D. W. Denning**. 2005. Correlation between *in vitro* growth rate and *in vivo* virulence in *Aspergillus fumigatus*. Medical Mycology. **43:**397-401.

32. **Pan, F., M. Jackson, Y. Ma, and M. McNeil**. 2001. Cell wall core galactofuran synthesis is essential for growth of mycobacteria. J. Bacteriol. **183:**3991-3998.

33. **Patterson, T. F.** 2006. Treatment of invasive aspergillosis: Polyenes, echinocandins, or azoles? Med Mycol. **44 Suppl 1:**357-362.

34. **Pedersen, L. L. and S. J. Turco**. 2003. Galactofuranose metabolism: a potential target for antimicrobial chemotherapy. Cell Mol. Life Sci. **60:**259-266.

35. **Perea, S., G. Gonzalez, A. W. Fothergill, W. R. Kirkpatrick, M. G. Rinaldi, and T. F. Patterson**. 2002. In vitro interaction of caspofungin acetate with voriconazole against clinical isolates of Aspergillus spp. Antimicrob. Agents Chemother. **46:**3039-3041.

36. **Pontecorvo, G., J. A. Roper, L. M. Hemmons, K. D. MacDonald, and A. W. Bufton**. 1953. The genetics of *Aspergillus nidulans*. Adv. Genet. **5:**141-238.

37. **Punt, P. J. and C. A. van den Hondel**. 1992. Transformation of filamentous fungi based on hygromycin B and phleomycin resistance markers. Methods Enzymol. **216:**447-457.

38. **Reichard, U., S. Büttner, H. Eiffert, F. Staib, and R. Rüchel**. 1990. Purification and characterisation of an extracellular serine proteinase from *Aspergillus fumigatus* and its detection in tissue. J. Med. Microbiol. **33:**243-251.

39. **Reijula, K. E.** 1991. Two common fungi associated with farmer's lung: fine structure of *Aspergillus fumigatus* and *Aspergillus umbrosus*. Mycopathologia. **113:**143-149.

40. **Rementeria, A., N. López-Molina, A. Ludwig, A. B. Vivanco, J. Bikandi, J. Pontón, and J. Garaizar**. 2005. Genes and molecules involved in *Aspergillus fumigatus* virulence. Rev. Iberoam. Micol. **22:**1-23.

41. **Simenel, C., B. Coddeville, M. Delepierre, J. P. Latgé, and T. Fontaine**. 2008. Glycosylinositolphosphoceramides in *Aspergillus fumigatus*. Glycobiology. **18:**84-96.

42. **Stynen, D., J. Sarfati, A. Goris, M. C. Prévost, M. Lesourd, H. Kamphuis, V. Darras, and J. P. Latgé**. 1992. Rat monoclonal antibodies against *Aspergillus* galactomannan. Infect. Immun. **60:**2237-2245.

43. **Suzuki, E., M. S. Toledo, H. K. Takahashi, and A. H. Straus**. 1997. A monoclonal antibody directed to terminal residue of beta-galactofuranose of a glycolipid antigen isolated from *Paracoccidioides brasiliensis*: cross-reactivity with *Leishmania major* and *Trypanosoma cruzi*. Glycobiology. **7:**463-468.

44. **Takayanagi, T., A. Kimura, S. Chiba, and K. Ajisaka**. 18-3-1994. Novel structures of N-linked high-mannose type oligosaccharides containing alpha-D-galactofuranosyl linkages in *Aspergillus niger* alpha-D-glucosidase. Carbohydr. Res. **256:**149-158.

45. **Takayanagi, T., K. Kushida, K. Idonuma, and K. Ajisaka**. 1992. Novel N-linked oligo-mannose type oligosaccharides containing an alpha-D-galactofuranosyl linkage found in alpha-D-galactosidase from *Aspergillus niger*. Glycoconj. J. **9:**229-234.

46. **Tanaka, N., M. Konomi, M. Osumi, and K. Takegawa**. 2001. Characterization of a *Schizosaccharomyces pombe* mutant deficient in UDP-galactose transport activity. Yeast. **18:**903-914.

47. **Toledo, M. S., S. B. Levery, B. Bennion, L. L. Guimaraes, S. A. Castle, R. Lindsey, M. Momany, C. Park, A. H. Straus, and H. K. Takahashi**. 2007. Analysis of glycosylinositol phosphorylceramides expressed by the opportunistic mycopathogen *Aspergillus fumigatus*. J. Lipid Res. **48:**1801-1824.

48. **Trejo, A. G., J. W. Haddock, G. J. Chittenden, and J. Baddiley**. 1971. The biosynthesis of galactofuranosyl residues in galactocarolose. Biochem. J. **122:**49-57.

49. **Wallis, G. L., R. L. Easton, K. Jolly, F. W. Hemming, and J. F. Peberdy**. 2001. Galactofuranoic-oligomannose N-linked glycans of alpha-galactosidase A from *Aspergillus niger*. Eur. J. Biochem. **268:**4134-4143.

50. **Weston, A., R. J. Stern, R. E. Lee, P. M. Nassau, D. Monsey, S. L. Martin, M. S. Scherman, G. S. Besra, K. Duncan, and M. R. McNeil**. 1997. Biosynthetic origin of mycobacterial cell wall galactofuranosyl residues. Tuber. Lung Dis. **78:**123-131.

51. **Wing, C., J. C. Errey, B. Mukhopadhyay, J. S. Blanchard, and R. A. Field**. 7-11-2006. Expression and initial characterization of WbbI, a putative D-Gal*f*:alpha-D-Glc beta-1,6-galactofuranosyltransferase from *Escherichia coli* K-12. Org. Biomol. Chem. **4:**3945-3950.

52. **Yoshida, T., Y. Kato, Y. Asada, and T. Nakajima**. 2000. Filamentous fungus *Aspergillus oryzae* has two types of alpha-1,2-mannosidases, one of which is a microsomal enzyme that removes a single mannose residue from Man9GlcNAc2. Glycoconj. J. **17:**745-748.

53. **Zhuo, H., H. Hu, L. Zhang, R. Li, H. Ouyang, J. Ming, and C. Jin**. 28-9-2007. Protein O-mannosyltransferase 1 (AfPmt1p) in *Aspergillus fumigatus* is crucial for cell wall integrity and conidia morphology especially at an elevated temperature. Eukaryot. Cell.

FIGURE LEGENDS

Figure 1 A) Schematic representation of the chromosomal *glfA* locus in wild type, Δ*glfA* and reconstituted wild type *glfA**. Thick black bars show flanking regions used for homologous recombination. The positions of probes (1-3) used for Southern Blot along with respective restriction fragments (size in kb) are indicated. B) Southern Blots of genomic DNA digested with indicated restriction enzymes and hybridised to different digoxigenin-labeled probes. wt, wild type; *ble/tk*, phleomycin resistance/thymidine kinase fusion gene; P, promoter; T, terminator.

Figure 2 A) Western Blots of *A. fumigatus* mycelial extracts containing glycoproteins and cell wall polysaccharides stained with horseradish peroxidase conjugates of either Gal*f*-specific mAb EB-A2 (left) or α-mannose binding lectin Concanavalin A (right). B) *A. fumigatus* GIPCs separated by High Performance Thin Layer Chromatography and stained with Gal*f*-specific mAb MEST-1 (left) or orcinol (right). White bars indicate the origin.

Figure 3 A) Electropherograms of fluorescently labeled N-glycans enzymatically released from secreted *A. fumigatus* glycoproteins. Oligosaccharides from wt and Δ*glfA* were either untreated (panels 1 and 2), digested with *T. reesei* α1,2-exomannosidase with or without hydrofluoric acid treatment (panels 3 to 6) or digested with Jack Bean α-mannosidase (panels 7 and 8). Bovine RNAse B N-glycans served as reference (panel 9). B) Structures of bovine RNAse B reference N-glycans. C) Major N-glycans found on *A. niger* α-galactosidase and α-glucosidase (44,45). Black squares, N-acetylglucosamine; grey circles, mannose; white pentagon, galactofuranose.

Figure 4 A) Colony morphology of *A. fumigatus* on minimal agar after two days. White bars represent 1 cm. B) Absolute and relative (compared to wild type) growth rates derived from three

independent experiments. P value from a t test indicates statistical significance (***, $P < 0.001$; ns, not significant).

Figure 5 Field emission scanning electron micrographs of cross-fractured mycelial walls of *A. fumigatus* wt and Δ*glfA*. Panel 1 and 3 display the highest measurement of cell wall thickness. Panel 2 and 4 present two measurements illustrating the 50% reduction of Δ*glfA* cell wall thickness.

Figure 6 A) Survival of immunosuppressed mice infected intranasally with *A. fumigatus* wt (continuous), Δ*glfA* (dotted) or *glfA** (dashed) and uninfected mice (dot-dashed). Each group consisted of 20 animals. B) Quantitative PCR determination of *A. fumigatus* burden (measured as conidial equivalents, see Material and Methods) in lung tissue from immunosuppressed mice infected with wt (continuous) or Δ*glfA* (dotted). Each datapoint represents mean values obtained from three to five animals. Error bars indicate standard error of the mean.

Figure 7 Periodic Acid Schiff stained lung sections of mice infected with *A. fumigatus* wild type (left), Δ*glfA* (middle) or *glfA** (right). Fungal colonies appear purple/red. Infected sites are typically surrounded by areas of necrotic tissue but show no or hardly any infiltrating leukocytes. The scale bar represents 100 µm.

TABLES

Table 1. DNA oligonucleotides used in this study.

Oligonucleotide	Sequence (5'->3'; restriction site underlined)	Description (Restriction site)
PS1	ATAAGCGGCCGCAAGCTGGGAACGCGATTCAA	5' flanking region pΔglfA reverse (NotI)
PS12	TATACCGCGGCTGCCAAGCTATCAGTTTCC	5' flanking region pΔglfA sense (SacII)
PS3	ATCCGGTGCTCAGGTATTCGCCA	3' flanking region pΔglfA sense (EcoRV)
PS4	ATCCATCGATCATATCCTATGCGGTCTCAG	3' flanking region pΔglfA reverse (ClaI)
PS66A	TTACGCATTCCCAGCAGTTG	Southern Blot probe 1 sense
PS67A	TGCGCTGTGATGAATGGTGT	Southern Blot probe 1 reverse
PS68A	TCCACAATACGTCCCCTACA	Southern Blot probe 2 sense
PS69A	GTATGAACCCTCTCCCAATG	Southern Blot probe 2 reverse
PS20	AAGGTCGTTGCGTCAGTCCA	Southern Blot probe 3 sense
PS21	TCGATGTGTCTGTCCTCC	Southern Blot probe 3 reverse
PS23s	ATGCCGCTCTCGAGGCTCGT	Site-directed mutagenesis *glfA** sense (XhoI)
PS23r	CACGAGCCTCGAGAGCGGCA	Site-directed mutagenesis *glfA** reverse (XhoI)
PS28	ATATGCGGCCGCAAACAGGAGCGAAGTAGT	5' flanking region pglfA* sense (NotI)
PS31	ATATCCCGGGAGTTTGGTGCTGTGGTAGGT	3' flanking region pglfA* reverse (XmaI)
PS78	CGTGTCTATCGTACCTTGTTGCTT	18S rRNA gene fragment sense
PS79	AACTCAGACTGCATACTTTCAGAACAG	18S rRNA gene fragment reverse
probe	**FAM**-CCCGCCGAAGACCCCAACATG-**TAMRA**[a]	qPCR hybridisation probe

[a]FAM, carboxyfluorescein; TAMRA, carboxytetramethylrhodamine.

Table 2. MICs of various antifungal agents against *A. fumigatus* mutants obtained from a broth microdilution assay.

Genotype	AmB[a]	Vor[b]	Cas[c]	NiZ[d]	H_2O_2[e]
			mg/L		
wt	3.9	0.3	62.5	500	218
Δ*glfA*	2.0	0.04	31.3	62.5-125	218
glfA*	3.9	0.3	62.5	500	218

[a]Amphotericin B (MIC90), [b]Voriconazole (MIC50),

[c]Caspofungin (MIC90), [d]Nikkomycin Z (MIC50),

[e]MIC100.

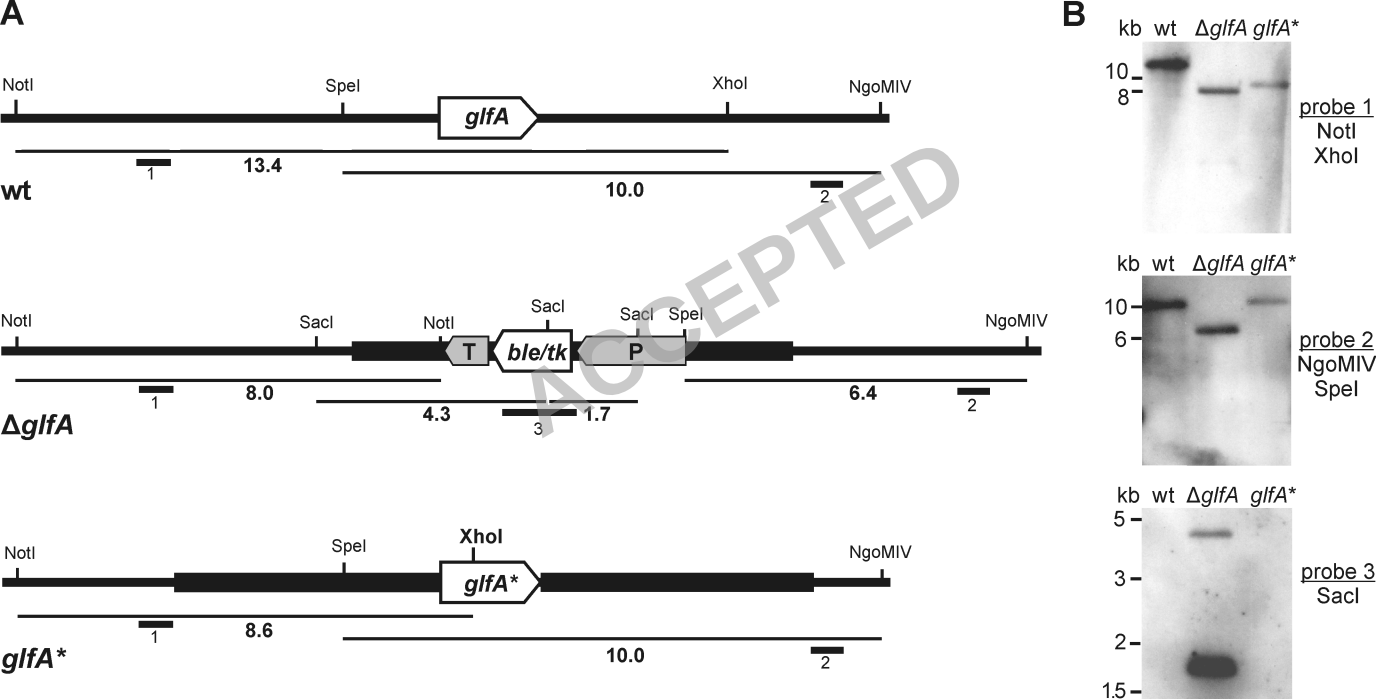
A
NotI
SpeI
glfA
XhoI
NgoMIV
1
13.4
10.0
2
wt
NotI
SacI
NotI
SacI
SacI
SpeI
NgoMIV
T
ble/tk
P
1
8.0
4.3
3
1.7
6.4
2
ΔglfA
NotI
SpeI
XhoI
glfA*
NgoMIV
1
8.6
10.0
2
glfA*
B
kb wt ΔglfA glfA*
10
8
probe 1
NotI
XhoI
kb wt ΔglfA glfA*
10
6
probe 2
NgoMIV
SpeI
kb wt ΔglfA glfA*
5
3
2
1.5
probe 3
SacI

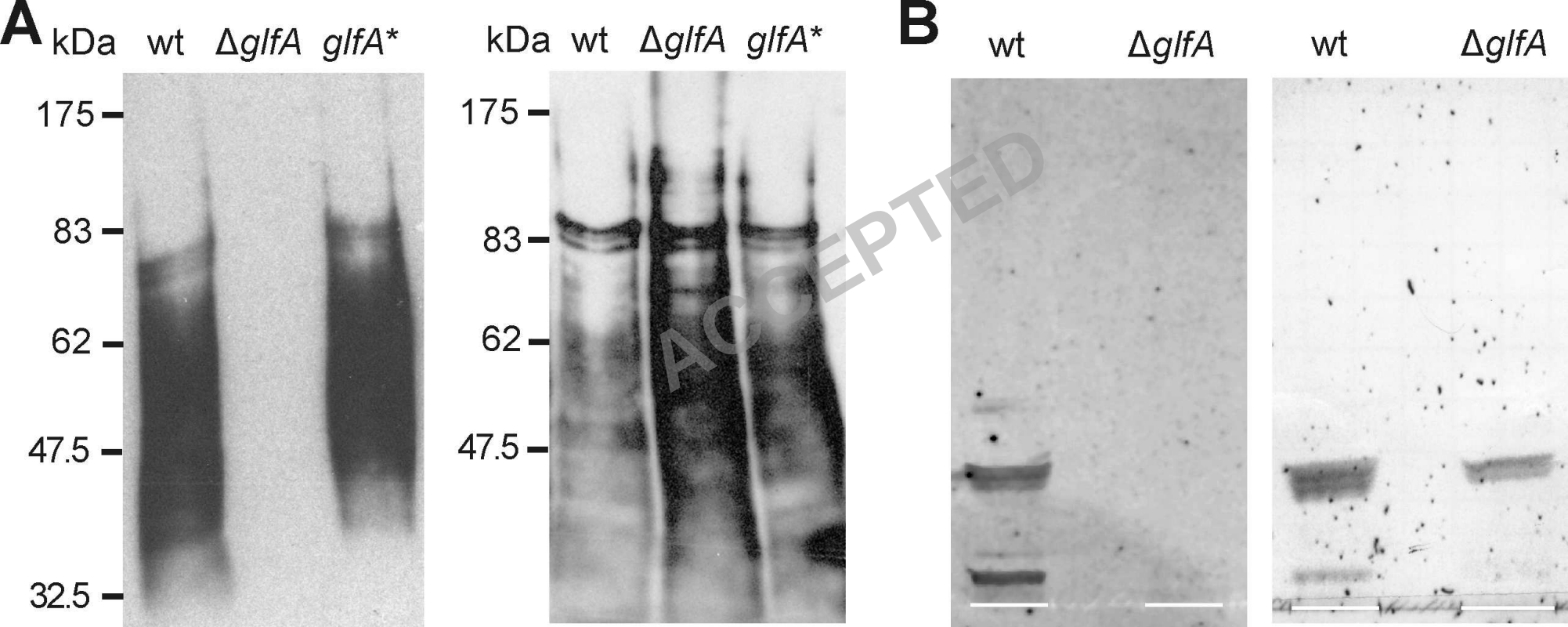
A
kDa
wt
ΔglfA
glfA*
175
83
62
47.5
32.5
kDa
wt
ΔglfA
glfA*
175
83
62
47.5
B
wt
ΔglfA
wt
ΔglfA

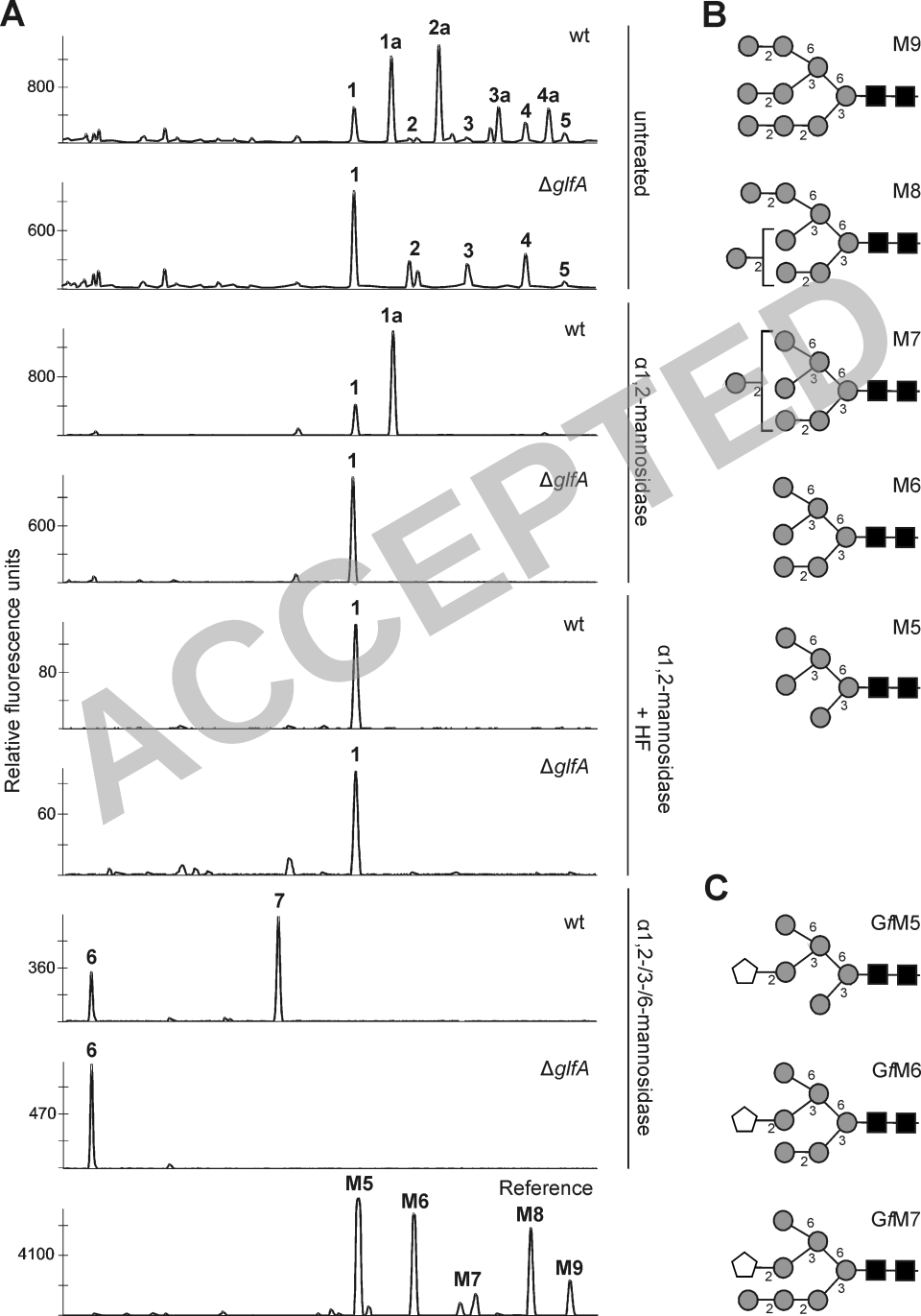
A
B
C
wt
ΔglfA
untreated
α1,2-mannosidase
α1,2-mannosidase + HF
α1,2-/3-/6-mannosidase
Reference
Relative fluorescence units
M9
M8
M7
M6
M5
GfM5
GfM6
GfM7
ACCEPTED

A

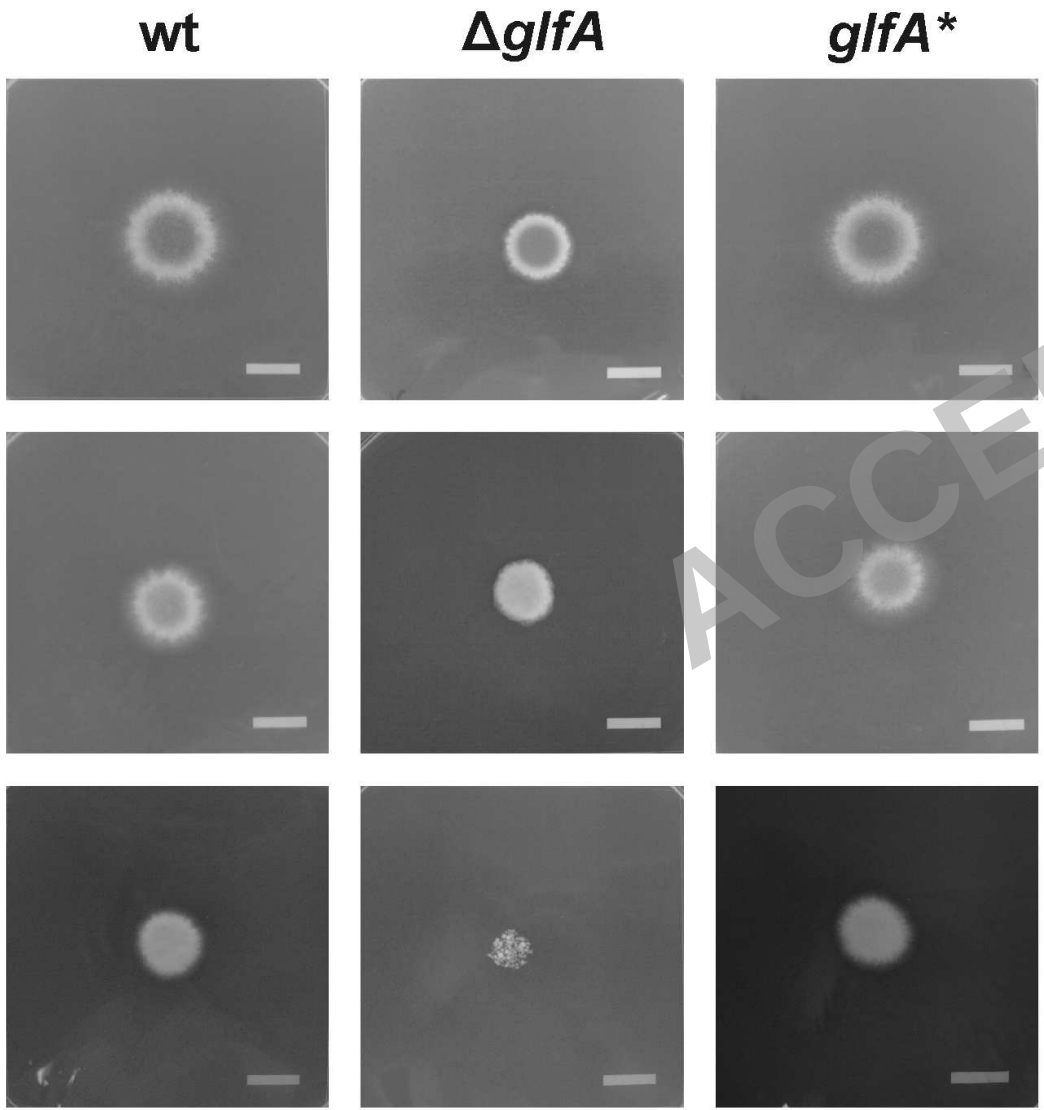

B

	Growth rate [µm/h]	rel.	P
37 °C			
wt	654	1	
Δ*glfA*	270	0.41	***
*glfA**	670	1.02	ns
42 °C			
wt	546	1	
Δ*glfA*	137	0.25	***
*glfA**	536	0.98	ns
47 °C			
wt	235	1	
Δ*glfA*	68	0.29	***
*glfA**	257	1.09	ns

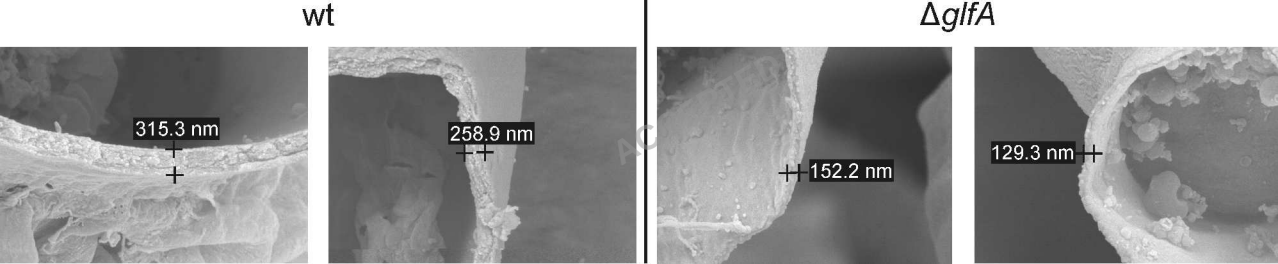
wt
ΔglfA
315.3 nm
258.9 nm
152.2 nm
129.3 nm

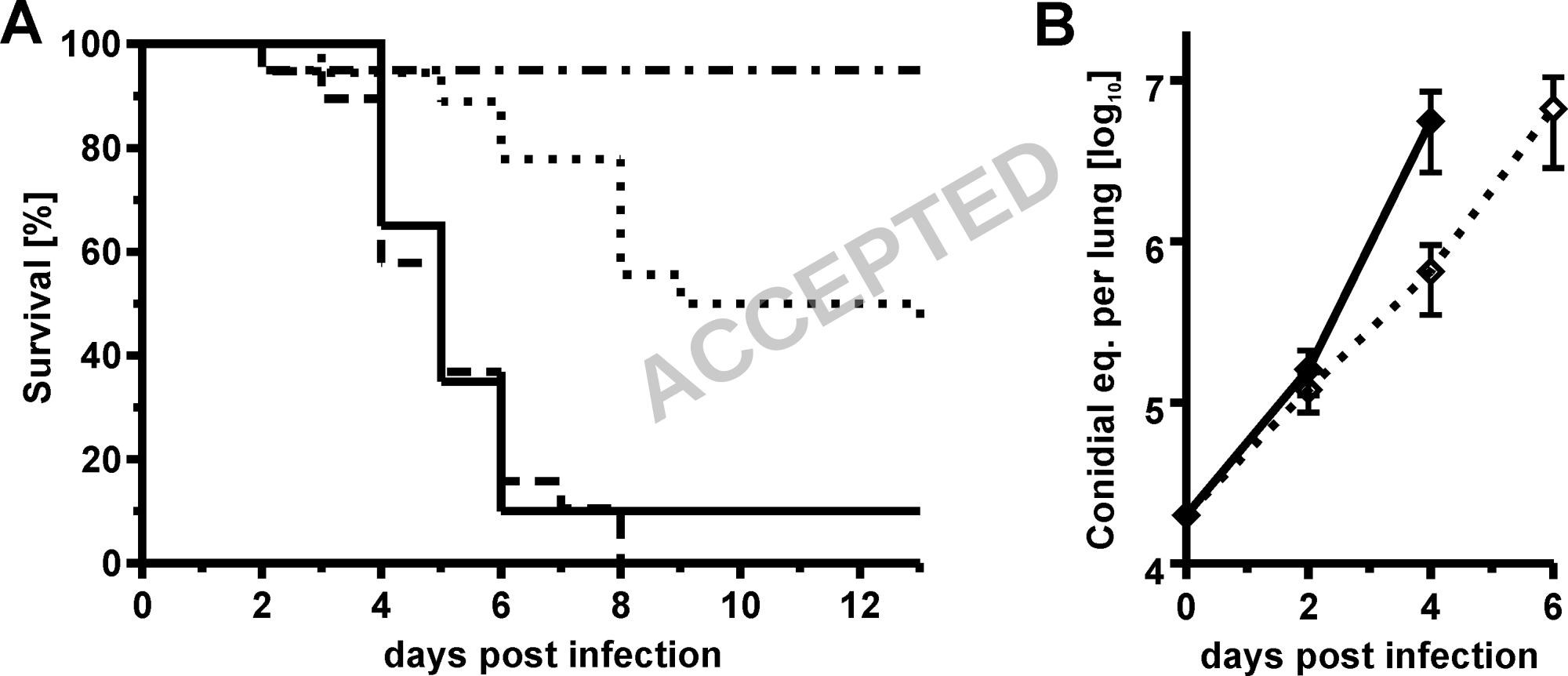
A
Survival [%]
100
80
60
40
20
0
0
2
4
6
8
10
12
days post infection
B
Conidial eq. per lung [log10]
7
6
5
4
0
2
4
6
days post infection

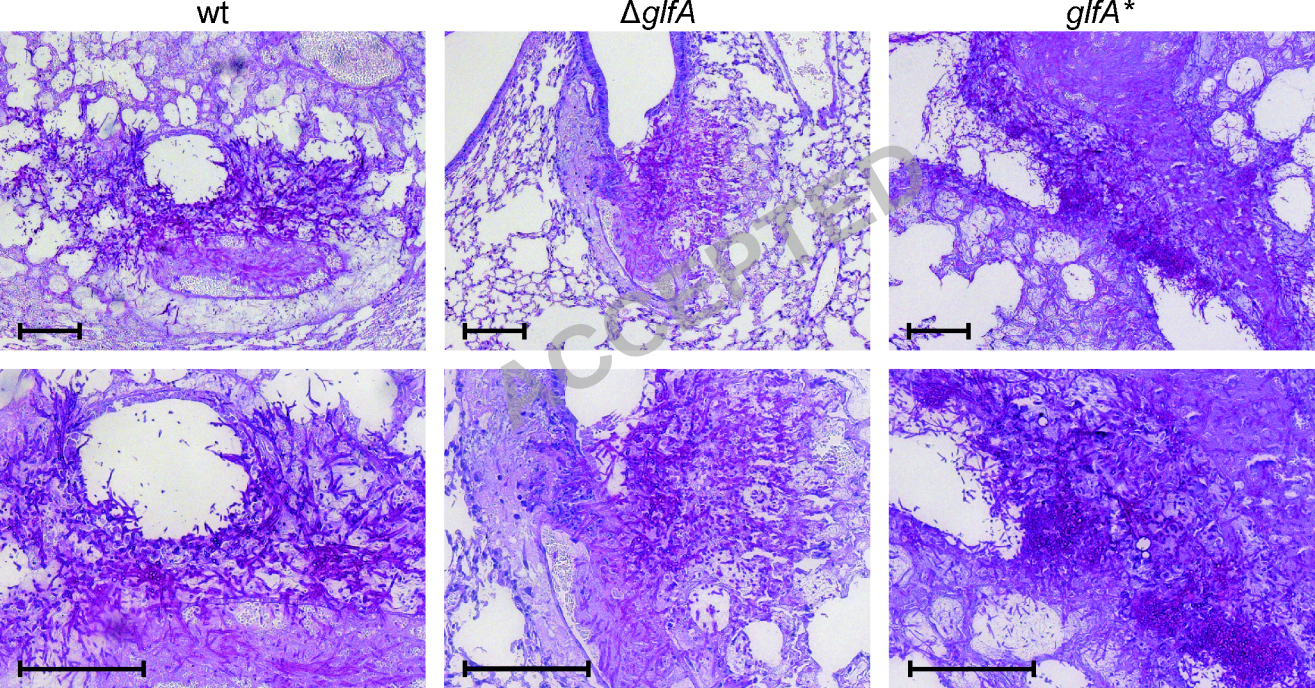
wt
ΔglfA
glfA*